Study of Constant DC-voltage Control for VIENNA Rectifier under No-load Condition

Weizhang Song, Yang Yang, Mengyu Du, Patrick Wheeler, *Fellow, IEEE*

***Abstract*—VIENNA rectifier has emerged as a promising topology for ac-dc power converter, but it has the problem of the dc-link output voltage surge under no-load condition. In this paper, a high reliability hardware auxiliary circuit and an easy-implement software regulation algorithm are proposed to achieve voltage stability. Firstly, voltage oriented current cross-decoupling control strategy is introduced and the reason of the voltage surge has been analyzed using equivalent circuit model. Secondly, the equivalent circuit model of different working state for auxiliary circuit in association with VIENNA rectifier are described, along with introducing the selection of device parameters in the auxiliary circuit. Meanwhile, the mechanism of two working mode in the software regulation algorithm are analyzed to make the VIENNA work in boost and buck mode to achieve dc-voltage stability. Finally, the feasibility and effectiveness of the proposed methods have been verified using experimental results. The proposed methods not only suppress the dc-voltage surge, but also exhibit a good performance in terms of supply-side power factor and dc-voltage in a VIENNA rectifier, meanwhile maintaining the system adaptability under circumstance of the load step.**

***Index Terms*— VIENNA rectifier, constant dc-voltage control, no-load control, auxiliary circuit**

I. Introduction

With the development of power electronics, higher requirements are put forward for the rectifiers. Pulse width modulated (PWM) rectifiers including two- and three-level unidirectional PWM rectifiers have advantages over diode bridge rectifiers because of low input current total harmonic distortion (THD) and controllable power factor[1-3]. Comparing with conventional unidirectional PWM rectifiers, three-phase VIENNA rectifier has many advantages of lower cost, lower current THD, no dead zone for switching signal lower[4-6], lower semiconductor device voltage stress, higher power density, and higher efficiency[7-9]. Due to these characteristics, VIENNA rectifier is widely used in telecommunication power systems, electric vehicle (EV) charging pile and wind turbine systems as well as power factor correction systems, where high-power density and low device voltage stresses are required [10-12].

The VIENNA rectifier belongs to the boost-type energy unidirectional flow topology family [13-15], which results in a controllable dc-link output voltage and low input current THD. However, in some special applications, such as battery charging equipment or EV charging piles, the output has no-load condition, which can cause a significant problem related to the output voltage surge. The reason of this phenomenon is that dc-link only the charging process occurs for the dc-link capacitors and there is no discharge circuit for capacitors. The output voltage surge would seriously hinder the VIENNA rectifier promotion application.

In order to solve the dc-link output-voltage surge of ac-dc converter under no/light-load conditions, some dc-voltage suppression methods have been proposed. These methods mainly use the addition of current shaping network and current injection device in the active three-phase circuit[16-19] and make the rectifier into an isolated topology[20, 21]. For the former method, Pejovic *et al* proposed a three-phase active rectifier applied current injection and a passive resistance emulator[16], which makes the system to operate within a wide range of the load current. This circuit does not need switches, there are many magnetic components, which increases the system cost. A rectifier composed of a diode bridge, three bidirectional switches and a current shaping network is proposed in [17], and two kinds of current shaping networks are introduced. The system shows promising results for rated load. However, it can operate under light load but exhibits poor system performance. Hartmann *et al* proposed to add an auxiliary circuit (flying converter cell, which is named FCC) and current injection device on the passive three-phase rectifier [18,19]. The working principle of FCC is analyzed in [18]. [19] presented the working principle under no/light-load condition based on passive rectifier system employing FCC. However, this auxiliary circuit includes six power switches (IGBT), two electrolytic capacitors and two diodes via three inductors. The structure of topology and control method are relatively complex, increasing the difficulty of control and hardware costs. Furthermore, the isolated rectifier circuit provides a solution. [20] presents the design and optimization of a high performance isolated three-phase ac-dc converter, which is composed of VIENNA rectifier and LLC resonant circuit. [21] presented an isolated single-stage three-phase buck-type rectifier lies in the modification of the original VIENNA Rectifier III. These isolated rectifier topologies can maintain good system performance under light load. Whether it works under no-load conditions is not mentioned. In addition, because isolated topology needs transformers, more switches and other components, the cost also increases and control is difficult.

Some algorithmic solutions have also been used to solve this problem [22-26]. First, adaptive controller is a straightforward solution to resolve this issue, which is realized by employing a hysteresis control based on the introduction of a quasi-sinusoidal current reference and pulse width control in the

This study is supported by National Natural Science Foundation of China (51877176), Key Research and Development Program of Shaanxi Province (2021GY-293), Science and Technology Planning Project of Xi'an (22GXFW0085), the National Key Research and Development Program sub project (2023YFA1606801) *(Corresponding author: Weizhang Song.)*

Weizhang Song, Yang Yang and Mengyu Du are with the Department of Power Electronics and Motor, Xi'an University of Technology, Xi'an 710054, China. (e-mail: swz@xaut.edu.cn; 18092064658@163.com; 1312465984@qq.com).

Patrick Wheeler is with the Department of Electrical and Electronic Engineering, University of Nottingham, NG7 2RD Nottingham, U.K. (e-mail: pat.wheeler@nottingham.ac.uk).

standby power operation region [22]. However, additional controllers take up DSP resources, and parameters of controllers are also difficult to design. [23] proposed an improved burst-mode control, where the output of the voltage regulator is employed as the trigger. But this method needs to be implemented on the basis of a particular zero-order injection algorithm. Discontinuous conduction mode (DCM) also provide a solution. In [24], the VIENNA rectifier works in DCM and adjusts the duty cycle in real time to achieve stable dc-voltage. Leibl *et al* proposes to calculate duty cycle control scheme for VIENNA rectifier under light-load condition in DCM without relying on current measurements that leads to low THD of the input currents [25]. But the control of DCM is complex and it requires a lot of computational resources, which causes heavy calculation. [26] studies a pulse-skipping control to improve the efficiency of grid-tied inverter by taking the dc-voltage as the judging condition under light-load condition. But this strategy may raise the power grid flicker problem.

The major contribution of this paper is to present two methods with adding a hardware cost-saving and control-simplifying auxiliary circuit on the dc-link of VIENNA rectifier and an easy-implement constant dc-voltage control algorithm to ensure dc-voltage stability in VIENNA rectifier under no-load condition. The two methods only compare the dc-voltage and the given reference value to control the switch, and the control complexity is reduced. The difference is that the former controls the switches of the auxiliary circuit with fewer components when VIENNA works normally, which provide an energy flow loop to make the capacitor charge and discharge in the output and auxiliary circuit to maintain the dc-voltage stability. While in the latter, the bidirectional switches are controlled in normal or off operation to make the VIENNA work in boost and buck mode to achieve dc-voltage stability. The experimental results show that the two methods can all effectively achieve the constant dc-voltage control for VIENNA rectifier under no-load condition.

II. Double Closed Loop Control and Voltage Surge Reason for VIENNA Rectifier

A. Double Closed Loop Control algorithm and PWM strategy

Fig. 1 shows the circuit topology of the three-level VIENNA rectifier. The circuit is composed of a diode bridge and three bidirectional switches connecting the input phases to the dc-link neutral point. The three active switching units are controlled to ensure sinusoidal input current and a steady dc-voltage.

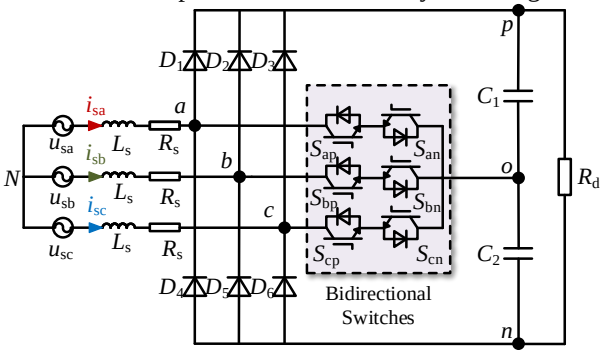

Fig. 1. VIENNA rectifier topology

As shown in Fig. 1, in the *d-q* coordinate system, the ac-side voltage balance equation of the VIENNA rectifier can be obtained as follows:

$$\begin{cases} L_s \dfrac{di_d}{dt} = -R_s i_d + \omega L_s i_q - u_d + u_{sd} \\ L_s \dfrac{di_q}{dt} = -R_s i_q - \omega L_s i_d - u_q + u_{sq} \end{cases} \tag{1}$$

where L_s is input filter inductor, R_s is the equivalent resistance of rectifier ac-side, ω is the fundamental wave angular frequency of input current, i_d and i_q are the input current in the *d-q* coordinates, u_{sd} and u_{sq} are the grid-side voltage in the *d-q* coordinates, u_d and u_q are the modulation voltage in the *d-q* coordinates.

It can be seen from (1) that there is mutual coupling between the *d-q* axis current. In order to eliminate coupling effects, the feed forward decoupling control of i_d and i_q is introduced, and the current cross-decoupling control is shown in Fig. 2. Meanwhile, the PI regulator is adopted as the current controller. The expression of the feed forward decoupling control is shown as follows:

$$\begin{cases} u_d = -(K_{iP} + \dfrac{K_{iI}}{s})(i_d^* - i_d) + \omega L_s i_q + u_{sd} \\ u_q = -(K_{iP} + \dfrac{K_{iI}}{s})(i_q^* - i_q) - \omega L_s i_d + u_{sq} \end{cases} \tag{2}$$

where K_{iP} and K_{iI} are the ratio and integral parameters of PI controller in current inner loop, and i_d^* and i_q^* are the given reference input current in *d-q* coordinates respectively.

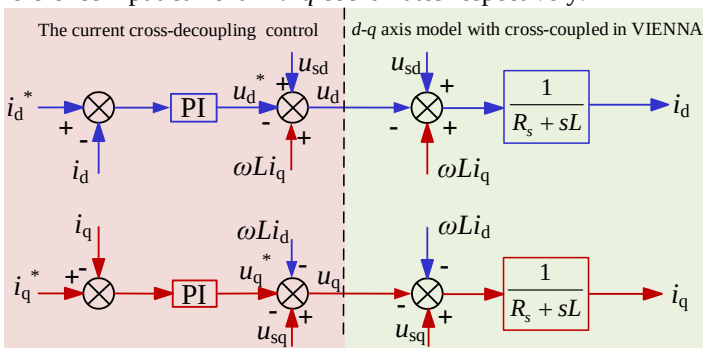

Fig. 2. Current cross-decoupling control block diagram

Substitute (2) into (1), the ac-side input voltage based on the *d-q* axis feed forward decoupling control can be described as follows:

$$\begin{cases} L_s \dfrac{di_d}{dt} + R_s i_d = (K_{iP} + \dfrac{K_{iI}}{s})(i_d^* - i_d) \\ L_s \dfrac{di_q}{dt} + R_s i_q = (K_{iP} + \dfrac{K_{iI}}{s})(i_q^* - i_q) \end{cases} \tag{3}$$

Comparing (1) with (3), it can be seen that there is a complete decoupling between the active current i_d and the reactive current i_q.

The current control loop is used to achieve ac-side power factor operation, so the given reference reactive current i_q^* is 0. Hence, it can be obtained:

$$\begin{cases} i_{\mathrm{d}}^{*} = (K_{\mathrm{iP}} + \dfrac{K_{\mathrm{iI}}}{s})(u_{\mathrm{dc}}^{*} - u_{\mathrm{dc}}) \\ i_{\mathrm{q}}^{*} = 0 \end{cases} \tag{4}$$

Meanwhile, the In-Phase Disposition (IPD) for VIENNA rectifier is selected as PWM strategy. Fig. 3 shows the modulation waveform of IPD. In Fig. 3(a), u_{c1} and u_{c2} are in-phase carriers, u_a is modulated wave in A-phase. In Fig. 3(b), g is the PWM wave generated by the carrier and modulated wave under modulation. Fig. 3(c) is the high-frequency output voltage pulse of the bridge arm of the VIENNA rectifier u_{ao}, which is equivalent to the reference voltage signal in the volt-second balance. u_{dc} is the dc-link voltage amplitude.

When u_a>0, the modulated wave is compared with the carrier u_{c1}. When the carrier wave is greater than the modulated wave, the switch is ON, and the output voltage of the bridge arm is connected to the point o through the switches, and the output voltage of the bridge arm is zero. When the carrier is less than the modulated wave, the switch is OFF. The voltage and current are in-phase, the bridge arm is connected to the point p through the diode, and the output voltage of the bridge arm is $+u_{dc}/2$. When u_a<0, vice versa.

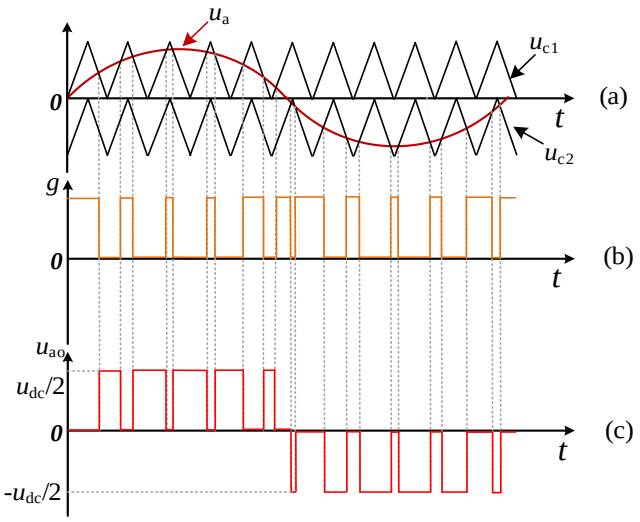

Fig. 3. Modulation waveform of In-Phase Disposition(IPD)

According to the above description, PWM strategy realizes the control of the pulse, and together with the double closed-loop based on the voltage oriented current cross-decoupling control realize the input and output control of the VIENNA rectifier, the system block diagram of which is shown in Fig. 4, where PI control strategy is included. The outer voltage loop is to track the dc-voltage and provide the command current value to the current loop. The inner current loop is to control the current according to the given reference current. The VIENNA rectifier can work under the unit power factor, and the dc-voltage can be stabilized to a given reference value.

B. Reason analysis for Dc-Voltage Surge under No-load Condition

The topology of the VIENNA rectifier can be equivalent to three single-phase boost converters in parallel [27-29]. Here, the reason for the dc-voltage surge under the no-load condition

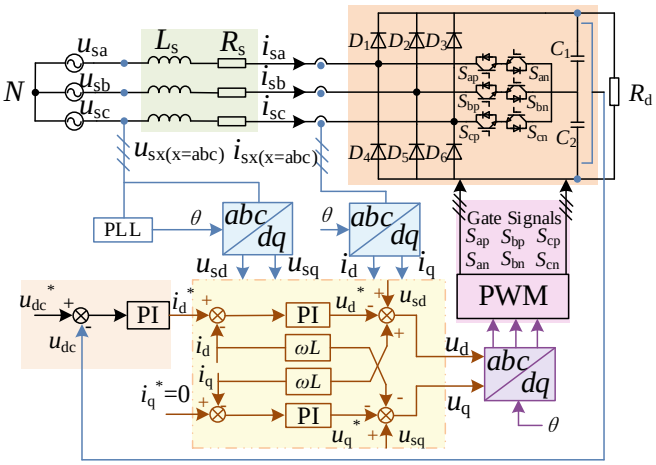

Fig. 4. Control system block diagram of double closed loops with voltage oriented current cross-decoupling control

in the case of A-phase is analyzed.

The equivalent circuit of A-phase for VIENNA rectifier is shown in Fig. 5(a), S_{ao} represents a bidirectional switch of A-phase. From Fig. 1 and Fig. 5(a), when the switch is ON, the VIENNA rectifier works in a normal multi-loop control state, and the equivalent circuit is shown in Fig. 5(b). The inductor L_s is charged by the power supply, which operates as a current source. When the switch S_{ao} is OFF, the VIENNA rectifier works in the diode rectifier state. The resulting dc-voltage source is composed of u_{ap} and u_{an}, which are equivalent voltage source u_{sa} and energy stored in inductor L_s. The equivalent circuit is shown in Fig. 5(c). Due to the diode, the energy of the converter is continuously transferred from the inductor to the dc-link capacitors, and the capacitors would be constantly charged by the power supply. Dc-voltage would be continuously increased owing to no discharge circuit for capacitors. Thus, there would be appeared a phenomenon that dc-voltage of VIENNA rectifier is subject to surge under no-load condition.

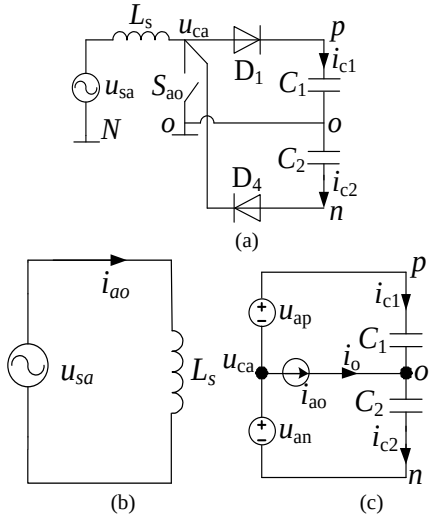

Fig. 5. Equivalent circuit of A-phase for VIENNA rectifier. (a) The equivalent circuit of A-phase topology. (b) The equivalent circuit of A-phase when S_{ao} is ON. (c) The equivalent circuit of A-phase when S_{ao} is OFF

Fig. 6 shows the simulation waveforms of input phase current, input phase voltage and dc-voltage without the constant dc-voltage control method. From the waveform, it can be seen the

dc-voltage cannot be maintained at constant value, which is out of control under no-load condition.

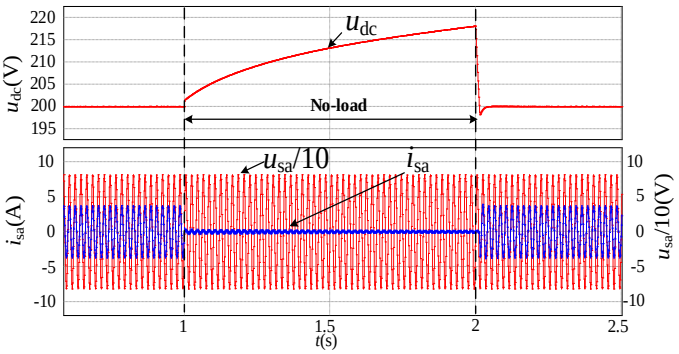

Fig. 6. Input phase voltage, phase current and dc-voltage simulation waveforms under no-load condition

When the value of dc-voltage exceed the given reference voltage stress of semiconductor device, it can cause damage to the switches and add additional magnetic device and switches conduction losses to the main power circuit. In addition, the high switch frequency would cause a lot of high frequency current ripple [30]. Moreover, during power supply access, capacitor charging can generate a large surge current, which damage rectifier devices and the voltage power source [31,32]. In order to solve this problem, two control methods are proposed in this paper to suppress dc-voltage surge of VIENNA rectifier, so as to maintain dc-voltage to be constant at a given value under no-load condition.

III. Constant Dc-voltage Control in a VIENNA Rectifier System under No-load Condition

A. Constant Dc-Voltage Method Based on Auxiliary Circuit for a VIENNA Rectifier under No-load Condition

A control method of VIENNA rectifier under no-load condition based on auxiliary circuit is presented in this sector, and VIENNA rectifier circuit employing the auxiliary circuit is shown in Fig. 7.

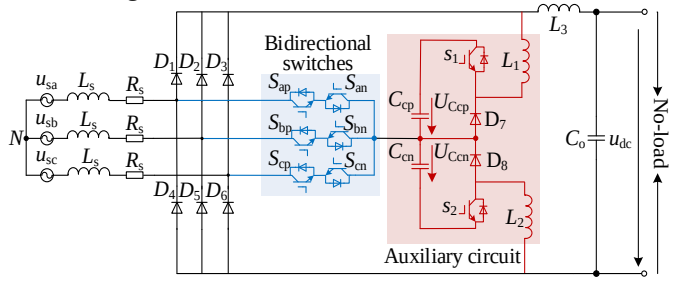

Fig. 7. VIENNA rectifier employing auxiliary circuit under no-load condition

The auxiliary circuit topology consists of two power switches (S_1 and S_2), two electrolytic capacitors (C_{cp} and C_{cn}) and two diodes (D_7 and D_8) and two inductors (L_1 and L_2). The positive and negative bus bars are connected to the outputs of the passive diode bridge (D_1-D_6) via three inductors (L_1-L_3). And two electrolytic capacitors (C_{cp} and C_{cn}) are connected to three bidirectional switches (S_{ap}-S_{cn}) via neutral points. Furthermore, two same capacitors (C_1 and C_2) are required on sides of the dc-link neutral-point for maintaining the balance of neutral-point voltage in VIENNA rectifier which is shown in Fig. 1. For the auxiliary circuit, the neutral-point is located in the middle of the auxiliary circuit, so the balance of neutral-point voltage depends on the auxiliary circuit, and the output capacitor (C_0) has function of the voltage regulation and filter. Therefore, dc-link only has the capacitor C_0 instead of C_1 and C_2. And the capacitor (C_{cp} and C_{cn}) in auxiliary circuit and dc-link (C_0) are exactly same.

Define the switching states of S_1 and S_2 in auxiliary circuit:

$$S_x = \begin{cases} 1, & S_x \text{ off}, \\ 0, & S_x \text{ on}, \end{cases} \quad x = 1, 2. \tag{5}$$

Each switch has two working states, 1 represents the switch is ON and 0 represents the switch is OFF. The two switches have the following four switching states: (0,0), (0,1), (1,0), (1,1), the diagram of which are shown in Fig. 8. Because the VIENNA rectifier is a three-level topology, when the voltage imbalance between the two capacitors, it will exacerbate the imbalance of the neutral-point, so that the voltage stress on the capacitor and the switch device is unevenly distributed. A large unbalance will hinder the system normal operation and even affect the system stability. Therefore, the normal working state of the auxiliary circuit are only (0,0), (1,1) two switching states.

Fig. 9 shows a schematic diagram of the dc-voltage and the switching signal waveforms of VIENNA rectifier employing auxiliary circuit under no-load condition. Fig. 9(a) shows the dc-voltage and the given reference voltage waveforms. The driving signals for the two power switches (S_1 and S_2) in the auxiliary circuit are shown in Fig. 9(b). In Figs. 9(c) and (d), the voltage waveforms of the dc-link capacitor C_0 and auxiliary circuit capacitors C_{cp} and C_{cn} are shown. Fig. 9(e) shows driving signal waveform of a switch (S_{ap}) of bidirectional switches in VIENNA rectifier.

The auxiliary circuit does not affect the work of the VIENNA rectifier, and the bidirectional switches are ON and OFF normally. Here, taking S_a=0, S_b=1, S_c=0 (switching states 010) as an example. The working principle of auxiliary circuit is shown in Fig. 10. In the sector I, the grid voltage $u_{sa}>u_{sb}>u_{sc}$, and $u_{sa}>0$, u_{sb}, $u_{sc}<0$ (Sector division and switching state are described in section III.B). The A- and C-phases switches are OFF, and the B-phase switch is ON. The current starts from A-phase, flows through D_1, L_3, C_0, L_1 and D_8, and flows back to B-phase through the bidirectional switches S_b and flows through D_1, L_3, C_0, then returns to C-phase through diode D_6. Note that i_{sa} i_{sb} i_{sc} in the figure are only the theoretical current flow. In

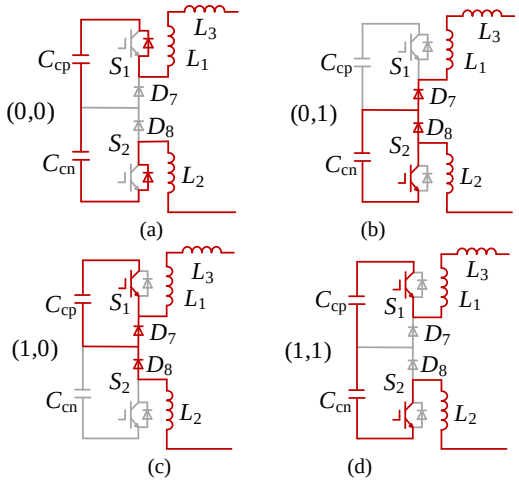

Fig. 8. Auxiliary circuit switching states diagram

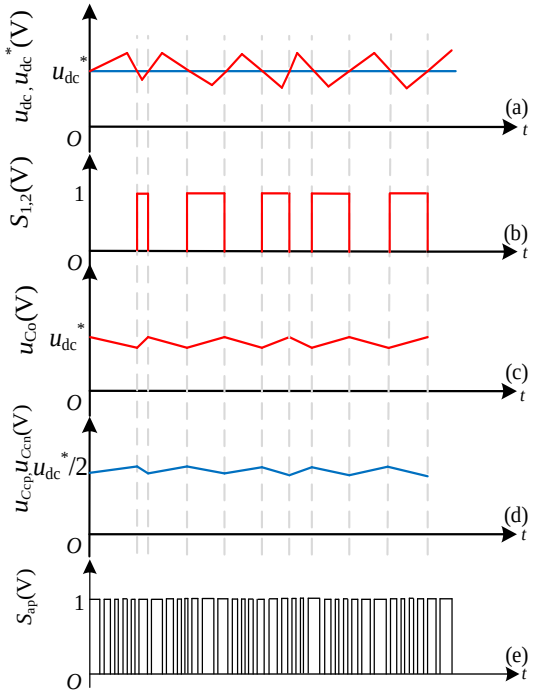

Fig. 9. The schematic diagram of dc-link capacitors voltage, switch signals and dc-voltage employing auxiliary circuit under no-load condition.

practice, the current amplitude in the circuit is almost 0 under no load condition.

As shown in Fig. 9(a) and Fig. 10(a), when the continuously dynamic measured value of dc-voltage (u_{dc}) is greater than the given constant reference voltage (u_{dc}^*), the switching state of S_1, S_2 in the auxiliary circuit is (0,0). The capacitor C_0, inductor L_1, L_2, L_3, the auxiliary capacitor C_{cp}, C_{cn} and the anti-parallel diode of the switches S_1, S_2 form a closed circuit. The C_0 provides energy to the C_{cn} and C_{cp} in the auxiliary circuit through the above circuit, the voltage of C_0 (u_{dc}) is decreased as shown in Fig. 10(c), and the voltage of capacitors C_{cp} and C_{cn} (u_{Ccp} and u_{Ccn}) are increased shown in Fig. 9(d). Capacitor C_0 releases excess energy through an auxiliary circuit, so that the value of the dc-voltage can be stabilized to a given value under no-load condition.

Similarly, when the u_{dc} is less than u_{dc}^* shown in Fig. 9(a), the switching state of S_1, S_2 in the auxiliary circuit is (1,1) as shown in Figs. 9(b) and 10(b). C_0, L_1, L_2, L_3, C_{cp}, C_{cn} and the auxiliary circuit switch S_1, S_2 work. The capacitors C_{cp}, C_{cn} in the auxiliary circuit provide energy to the capacitor C_0 in dc-side through the loop, and the voltage of capacitors C_{cp} and C_{cn} (u_{Ccp} and u_{Ccn}) are decreased shown in Fig. 9(d). The voltage of capacitor C_0 (u_{dc}) is increased shown in Fig. 9(c). The auxiliary circuit capacitors (C_{cp} and C_{cn}) continue to transfer energy to the capacitor C_0 through a flow path controlled by a signal as shown in Fig. 9(b), thus maintaining the value of dc-voltage at constant.

In addition, the switch (S_{ap}) signal of VIENNA rectifier is shown in Fig. 9(e), the VIENNA rectifier with auxiliary circuit does not affect the normal modulation process of its six switches (S_{ap}-S_{cn}).

According to above analysis, it can be seen that by constantly and frequently change the two switching states, the dc-voltage of the rectifier can be stabilized and output under no-load condition.

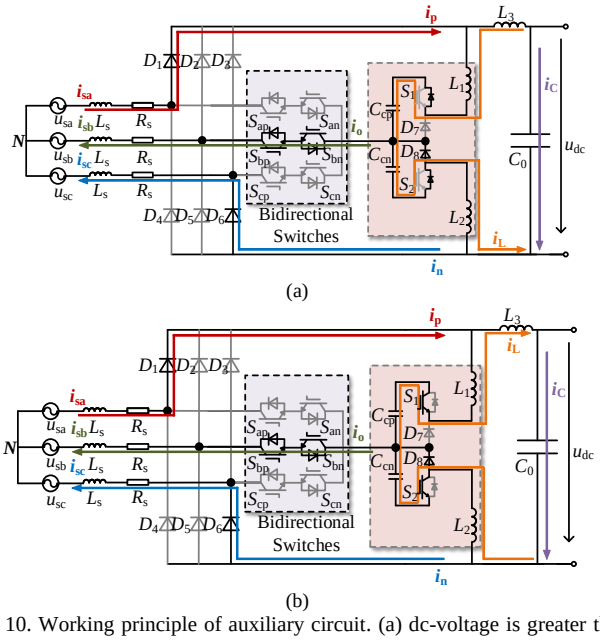

Fig. 10. Working principle of auxiliary circuit. (a) dc-voltage is greater than the given reference. (b) dc-voltage is less than the given reference.

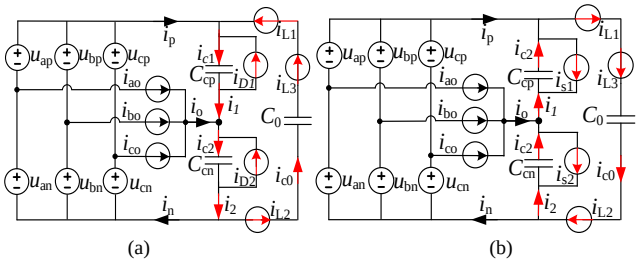

Fig. 11. Equipment circuit of VIENNA rectifier with auxiliary circuit. (a)dc-voltage is greater than the given reference. (b)dc-voltage is less than the given reference.

Fig. 11 shows the equivalent circuit diagram of VIENNA rectifier employing auxiliary circuit. The current source is controlled by using the switches, while the capacitor voltage is decided by the equivalent voltage source, including the inductor voltage. However, the inductor voltage is partly decided by the current source, so the capacitor voltage is indirectly controlled by the switches.

Thus, if the dc-voltage u_{dc} is greater than the given reference voltage u_{dc}^*, the equivalent circuit of VIENNA rectifier employing auxiliary circuit is shown in Fig. 11(a). The three bidirectional switches (S_{ap}-S_{cn}) works normally, while the two switches in the auxiliary circuit (S_1 and S_2) would be in ON state. The dc-link capacitor C_0 supplies energy to the auxiliary circuit capacitors (C_{cp} and C_{cn}) through three current sources equivalent to the three inductors (L_1-L_3), and reduces the voltage value of the dc-link capacitor C_0. The relationship between inductors and capacitors is shown as follows:

$$i_o = i_{L2} - i_{L1} = C_{cn}\frac{du_{Ccn}}{dt} - C_{cp}\frac{du_{Ccp}}{dt} \tag{6}$$

If the dc-voltage (u_{dc}) is less than the given reference voltage (u_{dc}^*), the equivalent circuit diagram of VIENNA rectifier employing an auxiliary circuit is shown in Fig. 11(b). The three bidirectional switches works normally, and the two switches (S_1 and S_2) in the auxiliary circuit would be in OFF state. The auxiliary circuit capacitors (C_{cp} and C_{cn}) supply energy to dc-link capacitor C_0 through the equivalent current sources of the

three inductors (L_1-L_3), and the voltage value of the dc-link capacitor C_0 increases. The dc-voltage can be stabilized at the given value by constantly high frequency alternating between two operations above. Therefore, the dc-link of VIENNA rectifier has a stable dc-voltage under no-load condition. The relationship between inductors and capacitors is shown as follows:

$$i_o = i_{L1} - i_{L2} = C_{cp}\frac{du_{Ccp}}{dt} - C_{cn}\frac{du_{Ccn}}{dt} \tag{7}$$

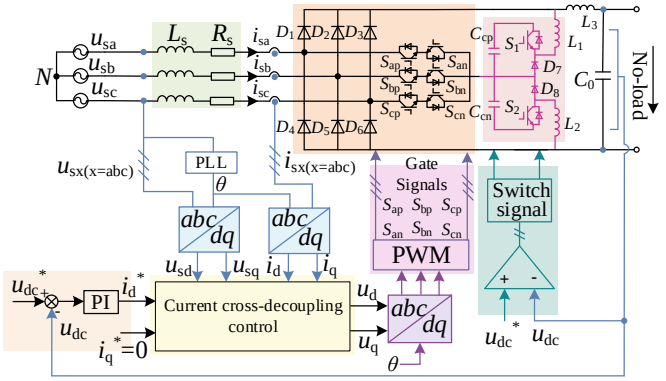

Fig. 12. Control system block diagram of constant dc-voltage control method employing the auxiliary circuit based on voltage oriented current cross-decoupling control for VIENNA rectifier under no-load condition.

The multi closed-loop control system control block diagram based on dc-voltage control of the VIENNA rectifier employing auxiliary circuit is shown in Fig. 12. Three bidirectional switches in the VIENNA rectifier, which is controlled by PI controller with voltage oriented current cross-decoupling control. The dc-voltage (u_{dc}) and the given reference voltage (u_{dc}^*) are sent to a comparator, whose output signal is used for driving two switches of the auxiliary circuit. They constantly works between ON and OFF state to control the dc-voltage of the VIENNA rectifier to be stabilized at constant, which preventing the dc-voltage surge under no-load condition.

B. Dc-Voltage Control Regulation Algorithm under No-load Condition

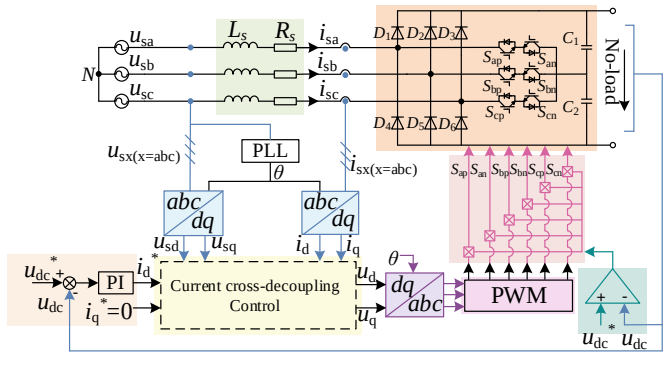

Fig. 13. Control system block diagram of constant dc-link voltage control regulation algorithm based on voltage oriented current cross-decoupling control for VIENNA rectifier under no-load condition.

Furthermore, the control regulation algorithm is proposed in this paper, the control system block diagram of which is shown in Fig. 13. The dc-voltage (u_{dc}) and the given reference voltage (u_{dc}^*) are sent to a comparator, and output value (0 or 1) are successively multiplied with the six PWM signals generated by

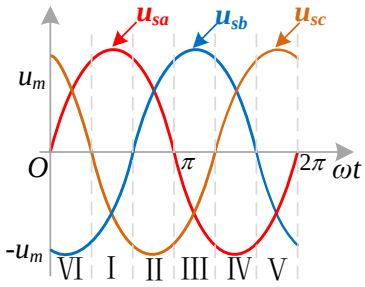

Fig. 14. Sector division

TABLE I
SWITCHING STATES

Power switch	Switch states							
S_a	0	0	0	0	1	1	1	1
S_b	0	0	1	1	0	0	1	1
S_c	0	1	0	1	0	1	0	1

the multi closed-loop control system shown in Fig. 13. The computation results are respectively used as driving signals for bidirectional switches of VIENNA rectifier. Hence, the dc-voltage can be maintained at a constant through two working states constantly high frequency alternating work.

In order to analyze the two working states mentioned above, three-phase input voltage (u_{sa}, u_{sb}, u_{sc}) are divided into 6 sections(I-VI) and each section is 60 degrees shown in Fig. 14.

Taking sector I (u_{sa}>0, u_{sb}<0, u_{sc}<0) as example, the three bidirectional switches have only two working states of the ON and OFF respectively. Thus, the power switches (S_{ap}-S_{cn}) of the VIENNA rectifier have 2^3=8 switch states, and 8 switching states are shown in TABLE I. Taking A-phase as an example, it is defined that the current outflow direction of on the grid-side as positive. When input voltage is in positive and the switch is ON, the switching function S_a = l, the gird-side current i_{sa} flows through the filter inductor L_s, the switches and inject dc capacitor neutral-point *o*. The inductor L_s is stores energy, and the current i_{sa} increases linearly. At this time, point *a* will be clamped to the neutral point *o*, and the voltage of the bridge arm u_{ao}=0. When the switch is OFF, the switching function S_a = 0, i_{sa} charges the dc capacitor through the bridge arm diode D_1. The inductor L_s releases energy, and supplies energy to the output side with the input side power supply. Then i_{sa} decreases, at this time point *a* will be clamped to point *p*, and the bridge arm voltage u_{ao}=u_{dc}/2. Similarly, when the input voltage is negative and the switch is ON, the switching function S_a = 1, point *a* will be clamped to the neutral point *o*, and the voltage of the bridge arm u_{ao}=0. If S_a = 0, point *a* will be clamped to point *n* and the voltage of the bridge arm u_{ao}=-u_{dc}/2.

Fig. 15 shows the two working modes of the equivalent circuit of the VIENNA rectifier when the dc-voltage is greater and less than the given reference under no-load condition. Noting that when the dc-voltage is less than the given reference, there are 8 switching states in one sector. Here taking the sector I and switching state 001 as example. Fig. 16 shows Flowchart of dc-voltage control regulation algorithm with cross-decoupling control under no-load condition. Part 1 is the voltage and current sampling and calculation of coordinate transformation, and this process is uninterrupted and continuous. Part 2 is to determine whether the dc-voltage is greater than the given reference voltage. Part 3 is double closed

loop control. Part 4 is PWM and part 5 is switch signal. Fig. 17 shows a schematic diagram of the dc-voltage and the switching signal of VIENNA rectifier using constant dc-voltage control algorithm under no-load condition. Fig. 17(a) shows the dc-voltage and the given reference voltage waveforms, and the voltage of the dc-link capacitor(C_1 and C_2) are shown in Fig. 17(b). Figs. 17(c) and (d) show the modulated wave (S_{cp} and S_{cn}). Fig. 17(e) shows the driving signals for the two power switching tubes (S_{cp} and S_{cn}). The main criterion of the regulation algorithm is whether the dc-voltage is less than the given reference value. The grid-side voltage and output dc-voltage need to be sampled. The former is to calculate the θ from PLL, and the latter is to determine whether the dc-voltage tracks the given reference value.

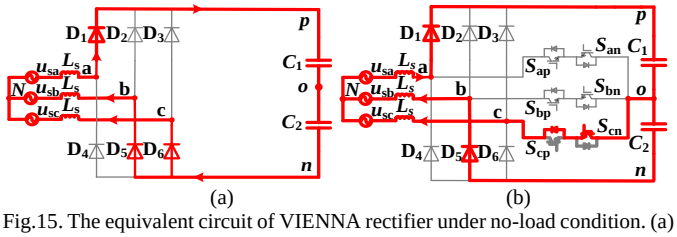

Fig.15. The equivalent circuit of VIENNA rectifier under no-load condition. (a) dc-voltage is great than the given reference. (b) dc-voltage is less than the given reference.

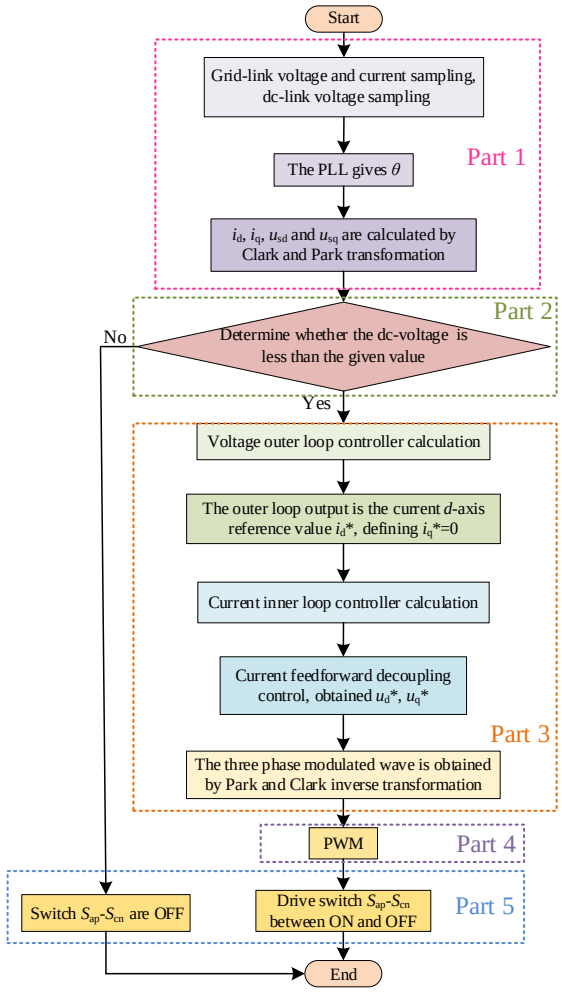

Fig. 16. Flowchart of dc-voltage control regulation algorithm with cross-decoupling control under no-load condition.

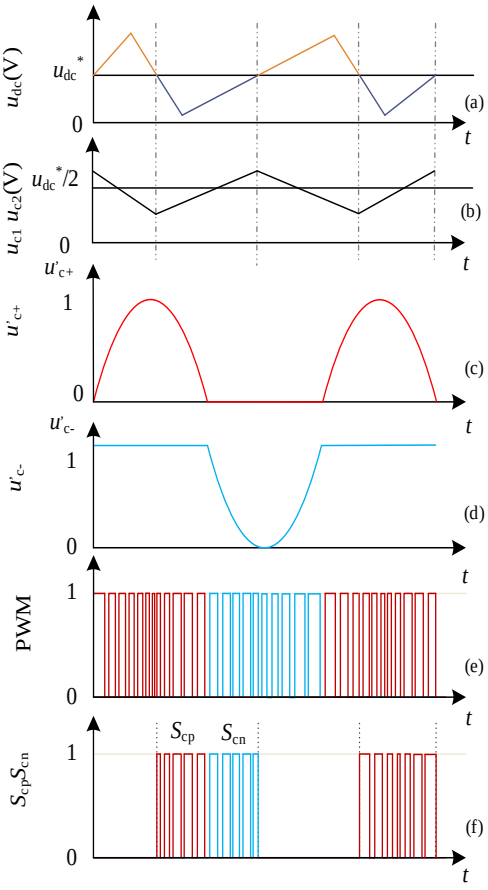

Fig. 17. Dc-voltage, capacitors voltage, dual modulated wave and switch signals waveforms using constant dc-voltage control algorithm under no-load condition.

As shown in Fig. 15(b) and 16, when the dc-voltage(u_{dc}) is less than the given reference voltage (u_{dc}^*), under the double closed-loop control (the part 3 in Fig. 16, including voltage oriented and current cross-decoupling), the VIENNA rectifier works in normally modulation state (take the switching state 001 as an example) and the six switches (S_{ap}-S_{cn}) work in high frequency (the part 4 and right of part 5 in Fig. 16). The dc-voltage of the VIENNA rectifier can track to the given reference by the closed-loop control. Since the terminal voltage u_{sx} of the switch is determined by the switching state and the current flow direction, S_a and S_b are OFF and S_c is ON when the switching state is 001. The power grid and inductor L_S charges the dc capacitor C_1 and C_2 through D_1, D_5, and S_c. The S_c bridge arm voltage can be equivalent to a controlled voltage source. There are modulated waves in S_{cn} and S_{cp} and the two switches interact. Due to the dual-carrier modulation, the direction of carrier modulation is opposite. The schematic diagram of modulate waves, PWM signal and switches drive (S_{cp} and S_{cn}) are shown in Figs. 17(c), (d), (e) and (f). Because it works in the VIENNA rectifier work mode, the equivalent voltage at the neutral point o can be calculated. The VIENNA rectifier features a boost characteristic, whose dc-voltage would be increased. The voltage value of capacitor C_1 and C_2 are same and dc-voltage would be increase.

As shown in Fig. 15(a) and 16, when dc-voltage (u_{dc}) is great than, the given reference voltage (u_{dc}^*), although the PWM

signal is present, the switching signal is directly blocked according to Fig. 13. The power switches (S_{cp} and S_{cn}) are OFF (the left of part 5 in Fig. 16), which are shown in Figs. 17(f). Only the diode provides the energy flow loop. At this time, if loss and voltage drop in diode is not considered. The dc-voltage should be the input line voltage envelope. Since the dc-voltage is greater than the maximum line voltage, the dc-voltage decreases without switch modulation and the dc-current is discontinuous. The following describes the working states of VIENNA rectifier without switch modulation under no-load condition.

Fig. 18 shows the voltage and current waveforms of the VIENNA rectifier works in current discontinuous of diode rectifier mode under no-load condition. When $\theta_1<\omega t<\theta_2$, the line voltage u_{ab} is greater than the dc-voltage u_{dc}, D_1 and D_5 works. i_{dc} increases from 0, and L_s stores energy. At the time of θ_2, u_{ab} is equal to u_{dc}. The L_s voltage is reduced to 0. i_{dc} reaches the maximum value. When $\omega t>\theta_2$, u_{ab} is less than u_{dc}. The energy stored in L_s is released to the load through D_1 and D_5. When $\omega t=\theta_3$, all the energy in L_s is released and the i_d is reduced to 0. When $\theta_4<\omega t<\theta_5$, u_{ab} is greater than u_{dc}, and D_1 and D_6 are worded. Each diode works twice in one on-cycle. At the time of θ_1 and θ_2, u_{ab} is equal to u_{dc}, then:

$$\theta_1=\sin^{-1}\left(\frac{u_{dc}}{\sqrt{2}u_{LL}}\right),\ \theta_2=\pi-\theta_1 \tag{8}$$

where u_{LL} is RMS value of line voltage.

When D_1 and D_5 works, the total voltage drop of the inductor voltage in the *a* and *b* phases is:

$$2L_s\frac{di_{dc}}{dt}=u_{ab}-u_{dc} \tag{9}$$

Then it can be further deduced:

$$\begin{aligned} i_{dc}(\theta)&=\frac{1}{2\omega L_s}\int_{\theta}^{\theta_1}(\sqrt{2}u_{LL}\sin(\omega t)-u_{dc})d(\omega t)\\ &=\frac{1}{2\omega L_s}(\sqrt{2}u_{LL}\cos\theta_1-\cos\theta)+u_{dc}(\theta_1-\theta)\end{aligned} \tag{10}$$

Substituting θ_2 into (10) the peak dc-current can be obtained as follows:

$$\hat{I}_{dc}(\theta)=\frac{1}{2\omega L_s}(\sqrt{2}u_{LL}\cos\theta_1-\cos\theta_2)+u_{dc}(\theta_1-\theta_2) \tag{11}$$

And the average value of dc-current:

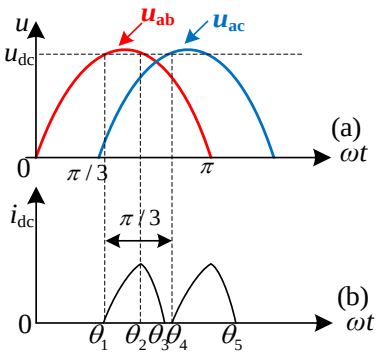

Fig. 18. The voltage and current waveforms of VIENNA rectifier works in current discontinuous of diode rectifier mode under no-load condition.

$$i_{dc}(\theta)=\frac{1}{\pi/3}\int_{\theta_1}^{\theta_3}i_{dc}(\theta)d(\theta) \tag{12}$$

When the u_{dc} decreases with the increase of the load current, and the decrease of u_{dc} makes the θ_3 and θ_4 in Fig. 18 close to each other. The i_{dc} will become continuous when the θ_3 and θ_4 overlap each other.

The VIENNA rectifier is alternated between two working states mentioned above to stabilize the dc-voltage at a constant, achieving the voltage control under no-load condition.

C. Comparison of proposed methods with other methods

The auxiliary circuit and regulation algorithm are described in section III.A and III.B, respectively. Both two methods can solve the problem of dc-voltage surge of VIENNA rectifier under no-load condition. In order to broaden the application field of the two algorithms, a comparison of two methods with other methods is described in this section.

The proposed auxiliary circuit consists of two switches, two capacitors, two inductors and two diodes. As described in section III.A, the switches will only appear in (1,1) and (0,0) switching states for the charge and discharge of the output and auxiliary capacitors, the clamp diode provides the circuit for the current, and the inductor is used for continuous current and output filtering. Comparing with addition of current shaping network and current injection device in [16-19] and isolated topology in [20,21]. Proposed auxiliary circuit in this paper with fewer components and simple controls realize the stability of dc-voltage under no-load condition. The two switches added to the auxiliary circuit merely provide an energy flow loop between the auxiliary circuit and the output capacitors instead of modulation, which simplifies control complexity. Comparison list of applicable circuit, auxiliary circuit cost, control complexity and whether no-load can be achieved are summarized in Table. II. Although this circuit is similar to the one proposed in [17-19], the modulation strategy of the bidirectional switches is completely different. In [17-19], The bidirectional switches work at low frequency to provide the injection circuit for the third harmonic current or in phase with the corresponding phase voltages and eliminate the dead zone of the current to ensures the sinusoidal current on the input side. The bidirectional switches in VIENNA rectifier operate at high frequencies for modulation, and it is not used for injection device. Meanwhile, compared with FFC topology in [17-19], the proposed method of auxiliary circuit can maintain the stability of dc-link voltage under no/light-load condition and there is no fluctuation in the voltage waveform, which doesn't affect the voltage boost performance of the system. Furthermore, since the neutral point is in the middle of the auxiliary circuit, the capacitor and switches of the two auxiliary circuit must be consistent. The auxiliary circuit can keep the balance of neutral-point voltage. In addition, VIENNA rectifier employing the auxiliary circuit has a low THD of input current which under rated load condition. It is precisely because of the capacitor that the dc-voltage is smoother at a given reference voltage fluctuation.

As for dc-voltage control regulation algorithm, comparing with hysteresis control [23] burst mode method based on a particular zero-order injection algorithm[24] and DCM with occupied DSP resources and computational burden [25,26], as

TABLE II.
COMPARISON LIST OF HARDWARE CIRCUIT METHOD

		Current injection and passive resistance proposed in [16]	Current injection and passive resistance proposed in [17]		Flying converter cell (FCC) proposed in [18,19]	VIENNA& LLC proposed in [20]	Three-phase buck-type rectifier proposed in [21]	The auxiliary circuit proposed in this paper
Applicable circuit		Three-phase active rectifier	Three-phase active rectifier		Three-phase active rectifier	VIENNA rectifier	VIENNA rectifier	VIENNA rectifier
Auxiliary circuit cost	Switch	/	/	/	6	6	4	2
	Diode	2	/	/	2	/	4	2
	Capacitor	1	2	2	2	2	/	2
	Inductor	1	/	/	3	2	/	2
	Transformer	2	/	1	/	1	1	/
	Resistor	2	3	2	/	/	/	/
Control complexity of switch in auxiliary circuit		/	/		Complex closed loop control	LLC resonance control	Coordinate control with rear stage bidirectional switches	Control to provide an energy flow loop
Whether no-load can be achieved		No, only light-load is considered	No, only light-load is considered		Yes	No, only light-load is considered	No, only light-load is considered	Yes

well as algorithm in [27] raise the power grid flicker problem. However, only the hysteresis control[23] and burst mode method[24] two methods can achieve no-load operation. Comparing with above algorithm, dc-voltage control algorithm proposed in this paper does not require additional circuits and control algorithms. And the algorithm is simple and easy to implement without a lot of calculation. Based on the voltage oriented current decoupling double closed-loop control, only the sampled dc-voltage is compared with the given value, and the voltage is stabilized by controlling the three bidirectional switches. In addition, because the switches work between modulation and off mode, the loss of the switches are reduced. Meanwhile, dc-voltage control algorithm not only has a stable voltage, but also has a low AC component of dc-voltage. And since no additional circuit, the size and cost of the system are reduced. Furthermore, the unbalance of neutral point is an inherent problem in three-level topology. To improve this problem, the neutral point voltage balance control algorithm based on injection zero sequence component is applied. Hence the output capacitance voltage can be maintained in balance. Due to the length limitation of the paper and the neutral point voltage balance algorithm is not the point of the discussion in this paper, so it is not shown here.

IV. AUXILIARY CIRCUIT DESIGN

In this section, the selection of inductors and capacitors for the auxiliary circuit is described.

A. Capacitors C_{cp}, C_{cn} of auxiliary circuit

For the VIENNA rectifier, two same capacitors (C_1 and C_2) are required in the dc-link neutral-point for maintaining the balance of neutral-point voltage in VIENNA rectifier. For the auxiliary circuit, the neutral-point is located in the middle of the auxiliary circuit, so the balance of neutral-point voltage depends on the auxiliary circuit. Therefore, dc-link only has the capacitor C_0 instead of C_1 and C_2. and the capacitor (C_{cp} and C_{cn}) in auxiliary circuit and dc-link (C_0) are exactly same in order to achieve voltage regulation.

As a filter, the capacitor is used to suppress the ripple of the dc-voltage, improve the voltage quality of the dc-link and stabilize the dc-voltage of the dc-link. As an energy storage component, the dc capacitor can store energy and assume the role of energy exchange between ac-dc. The design of the output capacitor is mainly considered from two aspects, one is to ensure the anti-interference performance of the VIENNA rectifier, and ensure that the dc-voltage overshoot is not large when the load changes. The larger capacitor, the stronger the anti-interference performance of VIENNA rectifier. The second is to ensure the rapid response of the dc voltage and ensure that the adjustment time of the dc-voltage will not be too long when the load changes. The smaller the output capacitor, the faster the dc voltage response. Based on the above, the value range of capacitor is obtained:

$$\frac{(u_{dc}-\Delta u_{max})^2 T_i}{2.4\Delta u_{max} u_{dc} R_d} \le C_0 \le \frac{t_r}{0.74 R_d} \tag{13}$$

where u_{dc} is dc-voltage, R_d is rated load, t_r is the rise time, T_i is the maximum inertial time constant of the system. Δu_{max} is the maximum dc-voltage ripple, which is 10% of the dc-voltage.

B. Inductor L_3 in dc-side

In the auxiliary circuit proposed in this paper, an output dc inductor is needed to suppress and maintain the dc output current because the capacitor of the auxiliary circuit has achieved the balance of the neutral-point. The output filter inductor can be designed according to the dc inductor current ripple.

The current flowing through the inductor L_3 is defined by the dc bus current i_{dc} and the 20% current ripple peak $\Delta i_{L,max}$:

$$L_3 \ge \frac{\sqrt{3} u_{dc}}{4\Delta i_{L,\max}} \left(\frac{1-M}{f_s}\right) \tag{14}$$

where f_s is switching frequency. M is modulation index and according to $M=3u_{in}/2u_{dc}$(u_{in}=100V, u_{dc}=200V), M=0.75. The maximum rated current i_{dc} is 12A, hence $\Delta i_{L,max}$ is 2.4A.

C. Inductor L_1 L_2 of auxiliary circuit

Considering that the auxiliary circuit is on both sides of the VIENNA neutral-point, the inductor on both sides must be consistent. Under light load/no-load conditions, the inductor needs to maintain an energy release loop in the dc-link and

auxiliary circuits, so the inductor current must be continuous. The minimum value of the inductor is bounded by continuous and discontinuous currents. The value of inductor can be obtained:

$$L_{1/2} \geq \frac{Mu_{dc}^{\ 2}(\frac{3}{4}M - \frac{1}{2\sqrt{3}})(1-\frac{\sqrt{3}}{2}M)}{P_{0,\min} f_s} \tag{15}$$

where $P_{0,\min}$ is the minimum output power, which is 7% of the rated output power(6kW).

V. Experiment Results

A power converter prototype was built to verify the validation of the proposed two dc-voltage control methods for VIENNA rectifier under no-load condition, which is shown in Fig. 19. The multi closed-loop control and dc-voltage control method were all carried out using a 32-bit DSP-type TMS320F2812 operating at a clock frequency of 150 MHz, and the experimental parameters are shown in TABLE III.

A. Experimental Waveforms of Voltage Control Regulation Based on Auxiliary Circuit under No-load Condition

Fig. 20 shows the waveforms of the constant dc-voltage control for the VIENNA rectifier employing the auxiliary circuit under no-load condition. Fig. 20(a) shows the average value of dc-voltage is stabilized at 200V under no-load condition. Because the designed logic value of switch driving signal in this experiment is contrary to the I/O interface output value of DSP (the high level of I/O output value indicates that the switch is OFF, vice versa). Thus, as seen from Fig. 20(a), the driving signal of the auxiliary circuit switch (S_1) is always maintained at 5V, which represents the two switches of the auxiliary circuit are always OFF. The input current of VIENNA rectifier is close to 0A, which verifies the validity of the constant dc-voltage control regulation for the VIENNA rectifier employing the auxiliary circuit under no-load condition.

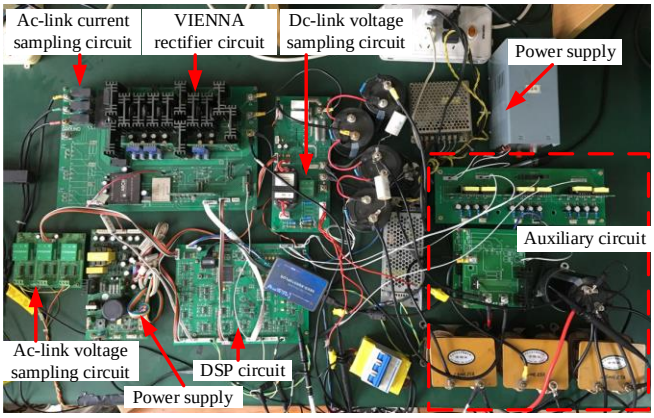

Fig. 19. Experimental prototype of VIENNA rectifier

TABLE III
System Parameters

Parameters	Value
Input line voltage RMS	100V/50Hz
Dc-link voltage reference	200V
Load resistor	90Ω/20kΩ
Switching frequency of S_{ap}-S_{cn}	4.8kHz
Ac-filter inductor	10mH
Dc-inductor	2.5mH
Dc-link filter capacitor	1650μF
Auxiliary circuit capacitor	1650μF
Auxiliary circuit inductor	2.5mH

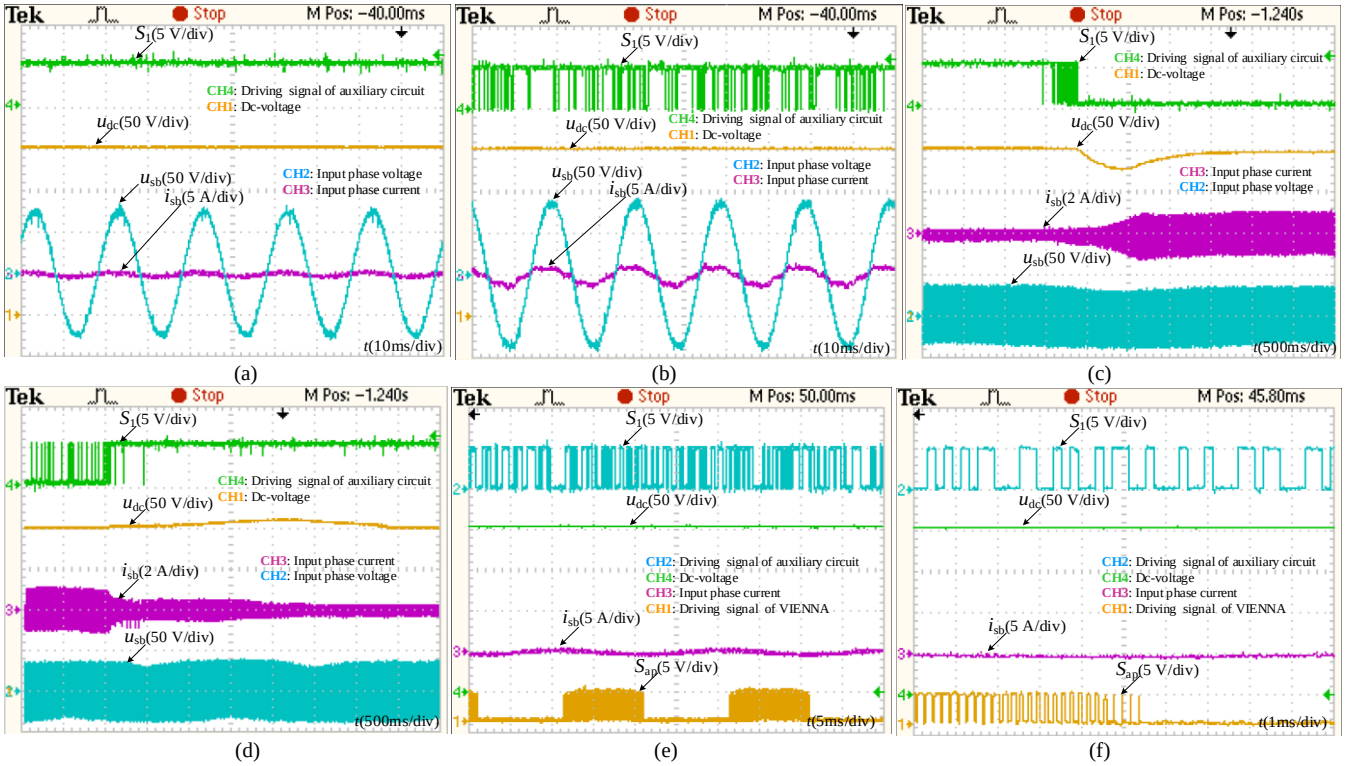

Fig.20. The proposed voltage control method employing auxiliary circuit under light/no-load conditions. (a) The steady-state waveforms under no-load condition. (b) The steady-state waveforms under light-load condition. (c) Response when steps from no-load to light-load. (d) Response when steps from light-load to no-load. (e) The switching signal waveforms of auxiliary circuit and bidirectional switch under no-load condition. (f) The amplifying waveforms of switching signals in the auxiliary circuit and bidirectional switch under no-load condition.

Fig. 20(b) shows the average value of dc-voltage is maintained at 200V under light-load (20kΩ) condition, the driving signal of the auxiliary circuit switch (S_1) is worked alternately in high frequency between ON and OFF state to maintain the value of dc-voltage at a constant, which is consistent with the theoretical analysis. It can be seen that the input phase current is in phase with the input voltage, which verifies the VIENNA rectifier has a good performance in power factor (PF) with the proposed auxiliary circuit method under light-load condition.

Figs. 20(c) and (d) show the dynamic response experiment waveform of input phase current, voltage, driving signal of switch S_1 and dc-voltage when the load stepped employing auxiliary circuit. The dc-voltage is maintained at a constant value even though the load is changed between light-load and no-load conditions. As shown in Fig. 20(c), it can be seen that the dc-voltage recovers to steady state within 1.5s under the condition of transient adding light-load from no-load. The driving signal of the auxiliary circuit switch (S_1) works alternately in high frequency between ON and OFF state under the condition of transient adding to the light-load and finally turning to ON state under light-load condition.

As shown in Fig. 20(d), it can be seen that the regulation time of dc-voltage is longer compared with Fig. 20(c). The reason is that the value of dc-voltage is raised under the condition of transient reducing to no-load from light-load, and the VIENNA rectifier does not exist a load circuit topology to consume energy of the dc-link capacitor. Hence, the voltage drop is slow and the regulation time is longer. The driving signal of the auxiliary circuit switch (S_1) is worked alternately in high frequency between ON and OFF state under the condition of transient reducing to no-load and turning to OFF state under no-load condition, which verifies the validity of constant dc-voltage control method for the VIENNA rectifier employing the auxiliary circuit under no-load.

Fig. 20(e) shows the experiment waveforms of a driving signal of the auxiliary circuit switch (S_1), a driving signal of bidirectional switch (S_{ap}), input phase current and dc-voltage under no-load condition. And Fig. 20(f) is the amplified waveforms of Fig. 20(e). As shown in Figs. 20(e) and (f), it can be seen that the logic of auxiliary circuit driving signal fully conforms to the theoretical analysis logic. The ON or OFF state of auxiliary circuit switches are depended on the output result from the comparator compared the dc-voltage and the given voltage value. As shown in Fig. 20(f), it can be seen that the waveform of S_{ap} is same with the theoretical analysis logic shown in Fig. 9(e), which indicates that the proposed constant dc-voltage control method employing the auxiliary circuit does not affect the normal operation of the bidirectional switches of the VIENNA rectifier. In addition, the switching frequency of the auxiliary circuit switch is much lower than that of the bidirectional switch. The amplitude of input phase current is about 0 A, which means that the switching loss is not large. And the average value of dc-voltage is stable at 200V, indicating that the application of auxiliary circuit is effective in suppressing the surge of dc-voltage of the VIENNA rectifier under no-load condition.

B. Experimental waveforms of Constant Dc-Voltage Control Algorithm under No-Load Condition

Fig. 21 shows the dynamic response waveform of input phase current and dc-voltage when steps from 100% load (90Ω) to no-load and recovers to 100% load without the constant dc-voltage control method. It can be seen that the dc-voltage is out of control under the condition of transient reducing to no-load, the value of dc-voltage increases rapidly to about 280V, appearing a phenomenon of dc-voltage surging in VIENNA rectifier. The dc-voltage amplitude is reduced under the condition of transient adding load, and the dc-voltage is recovered to constant after a short time adjustment. In addition, input phase current is also changed under the condition of transient changing load.

Fig. 21. Input phase current and dc-voltage when steps from 100% load to no-load and recovers to 100% load without the constant dc-voltage control algorithm.

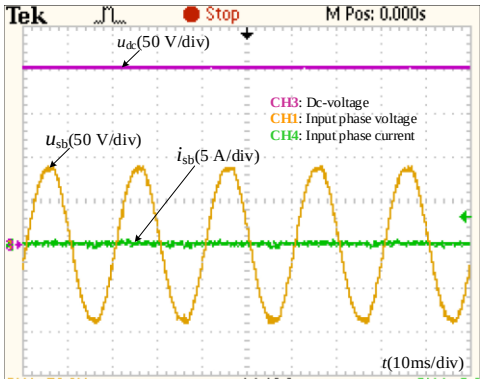

(a)

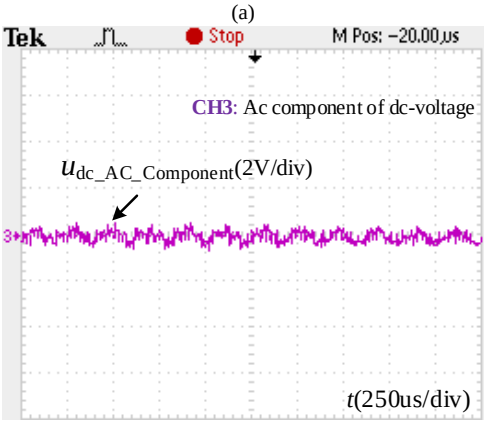

(b)

Fig. 22. The constant dc-voltage control algorithm under no-load condition (a) Input and output waveforms (b) Ac component of dc-voltage

Fig. 22 shows the waveform of input phase voltage, current , dc-voltage and its AC component of the VIENNA rectifier with the constant dc-voltage control algorithm under no-load condition. It can be seen that the amplitude of input phase current is about 0A and the average value of dc-voltage is maintained at 200V, indicating that the dc-voltage is still stable at the given value under no-load condition, which verified the effectiveness of the proposed constant dc-voltage control algorithm. In addition, it has a low dc-voltage AC component shown in Fig. 22(b).

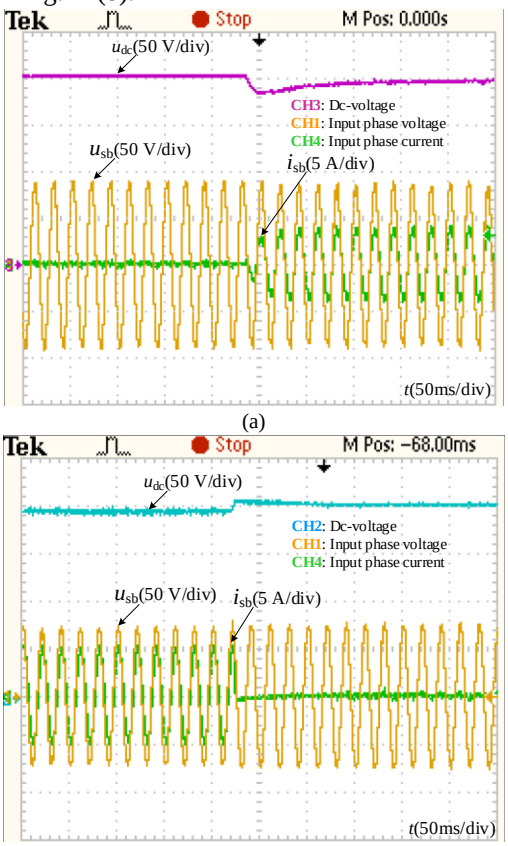

Fig. 23. Input phase voltage, current and dc-voltage with the proposed constant dc-voltage control regulation algorithm for VIENNA rectifier under no-load condition. (a) Response when steps from no-load to 100% load. (b) Response when steps from 100% load to no-load.

Fig. 23 shows the dynamic response experiment waveforms of input phase voltage, current and dc-voltage when steps from no-load to 100% load and steps from 100% load to no-load. From the waveforms, the dc-voltage is maintained at a constant even though the load changing. In Fig. 23(a), it can be seen that the dc-voltage recovers to steady state within about 8 basis wave cycles under the condition of transient adding to 100% load from no-load. In Fig. 23(b), it can be seen that the dc-voltage recovers to steady state within about 5 basis wave cycles under the condition of transient reducing to no-load from 100% load. It verified the good performance in dynamic properties of the proposed constant dc-voltage control algorithm for the VIENNA rectifier under no-load condition.

VI. Conclusion

This paper has presented two constant dc-voltage control methods with employing an auxiliary circuit and a software control algorithm based on cross-decoupling control strategy to solve the problem of the dc-link output voltage surging in a VIENNA rectifier under light/no-load conditions. The constant dc-voltage in VIENNA rectifier system is achieved depend on the capacitor charge and discharge two working states of auxiliary circuit and two working models of boost and buck mode in the VIENNA rectifier by proposed algorithm under no-load conditions. Moreover, the dc-voltage can be always maintained at a constant value by using these two methods when load steps between 100% load and no-load condition. In addition, the system after being added the proposed methods still exhibits the good performance in supply-side power factor as well as the fast response capability to load disturbance, meanwhile improving the adaptability of the load condition and broadening the engineering application for VIENNA rectifier.

References

[1] T. Friedli, M. Hartmann and J. W. Kolar, "The Essence of Three-Phase PFC Rectifier Systems—Part II," *IEEE Trans. Power Electron.,* vol. 29, no. 2, pp. 543-560, Feb. 2014.

[2] F. Wu and J. Zhao, "Current Similarity Analysis-Based Open-Circuit Fault Diagnosis for Two-Level Three-Phase PWM Rectifier," *IEEE Trans. Power Electron.,* vol. 32, no. 5, pp. 3935-3945, May 2017.

[3] W. Song, F. Xing, H. Yan, *et al*, "A Hybrid Control Method to Suppress the Three-Time Fundamental Frequency Neutral-Point Voltage Fluctuation in a VIENNA Rectifier ," *IEEE J. Emerg. Sel. Topics Power Electron.,* vol. 4, no. 2, pp. 468-480, Jun. 2016.

[4] Y. Ming, Y. Zhou, Y. Xing, *et al.,* "A Hybrid Carrier-Based DPWM With Controllable NP Voltage for Three-Phase Vienna Rectifiers," *IEEE Trans. Transp. Electrific.*, vol. 8, no. 2, pp. 1874-1884, Jun. 2022.

[5] L. Song, S. Duan, R. Li, *et al*, "A Hybrid Discontinuous PWM Strategy for Current Ripple and Neutral-Point Fluctuation Reduction of Parallel Vienna Rectifier," *IEEE Trans. Ind. Electron.,* vol. 70, no. 3, pp. 2531-2542, Mar. 2023.

[6] M. Rasouli, M. Shekari, H. Ghoreishy, *et al*. "Virtual Flux Direct Power Control for Vienna Rectifier Under Unbalanced Grid," *IEEE Trans. Power Electron.,* vol. 38, no. 7, pp. 8115-8125, July 2023.

[7] H. Zhang, C. Zhang, X. Xing, *et al*, "Three-Layer Double-Vector Model Predictive Control Strategy for Current Harmonic Reduction and Neutral-Point Voltage Balance in Vienna Rectifier," *IEEE Trans. Transp. Electrific.*, vol. 8, no. 1, pp. 251–262, Mar. 2022.

[8] W. Song, Y. Yang, Z. Jiao, *et al.*, "Simplified Model Predictive Current Control Based on Fast Vector Selection Method in a VIENNA Rectifier," *IET Power Electron.*, vol. 16, no. 3, pp: 436– 446, 2023

[9] D. Molligoda, S. Ceballos, J. Pou, *et al.*, "Hybrid Modulation Strategy for the Vienna Rectifier," *IEEE Trans. Power Electron.,* vol. 37, no. 2, pp. 1283-1295, Feb. 2022.

[10] M. Zhang, Y. Yuan, X. Sun, *et al*, "Harmonic Resonance Suppression Strategy of the Front-End Vienna Rectifier in EV Charging Piles," *IEEE Trans. Power Electron.,* vol. 38, no. 1, pp. 1036-1053, Jan. 2023.

[11] A. P. Monteiro, C. B. Jacobina, F. A. d. C. Bahia *et al*, "Vienna Rectifiers for WECS Applications with Open-End Winding PMSM," *IEEE Trans. Ind. Appl.,* vol. 58, no. 2, pp. 2268-2279, Mar. -Apr. 2022.

[12] W. Song, Y. Yang, Z. Jiao, *et al*, " Simplified Model Predictive Current Control Based on Fast Vector Selection Method in a VIENNA Rectifier," *IET Power Electron.*, vol. 16, no. 3, pp: 436– 446, Feb. 2023.

[13] J. D. V. Wyk, F. C. Lee, "On a Future for Power Electronics," *IEEE J. Emerg. Sel. Topics Power Electron.*, vol. 1, no. 2, pp. 59-72, Jun. 2013.

[14] J. Adhikari, I. V. Prasanna, S. K. Panda, "Reduction of Input Current Harmonic Distortions and Balancing of Output Voltages of the Vienna Rectifier Under Supply Voltage Disturbances," *IEEE Trans. Power Electron.,* vol. 32, no. 7, pp. 5802-5812, Jul. 2017.

[15] J. -H. Park, J. -S. Lee and K. -B. Lee, "Sinusoidal Harmonic Voltage Injection PWM Method for Vienna Rectifier with an LCL Filter," *IEEE Trans. Power Electron.* vol. 36, no. 3, pp. 2875-2888, Mar. 2021.

[16] Z P. Pejovic, P. Bozovic and D. Shmilovitz, "Low-harmonic, three-phase rectifier that applies current injection and a passive resistance emulator," *IEEE Power Electronics Letters*, vol. 3, no. 3, pp. 96-100, Sept. 2005.

[17] P. Pejovic, "A novel low-harmonic three-phase rectifier," *IEEE Transactions on Circuits and Systems I: Fundamental Theory and*

Applications, vol. 49, no. 7, pp. 955-965, July 2002.

[18] M. Makoschitz, M. Hartmann, H. Ertl, "Control Concepts for Hybrid Rectifiers Utilizing a Flying Converter Cell Active Current Injection Unit," *IEEE Trans. Power Electron.,* vol. 32, no. 4, pp. 2584-2595, Apr. 2017.

[19] M. Makoschitz, M. Hartmann and H. Ertl, "Analysis of a Three-Phase Flying Converter Cell Rectifier Operating in Light/No-Load Condition," in *2015 IEEE Applied Power Electron. Conf. Expo.* (APEC), Charlotte, NC, USA, 2015, pp. 92-100.

[20] Q. Wang, X. Zhang, R. Burgos, D. Boroyevich, A. White and M. Kheraluwala, "Design and optimization of a high performance isolated three phase ac/dc converter," *2016 IEEE Energy Conversion Congress and Exposition (ECCE)*, Milwaukee, WI, USA, 2016, pp. 1-10.

[21] S. Zhao, U. Borović, Marcelo Silva, et al., "Modified VIENNA Rectifier III to Achieve ZVS in All Transitions: Analysis, Design, and Validation," *IEEE Trans. Power Electron.,* vol. 36, no. 12, pp. 13404-13422, Dec. 2021

[22] N. C. Foureaux, J. H. Oliveira, F. D. De Oliveira, *et al*, " Command Generation for Wide-Range Operation of Hysteresis-Controlled Vienna Rectifiers," *IEEE Trans. Ind. Electron.,* vol. 51, no. 3, pp. 2373-2380, Jun. 2015.

[23] X. Tang, Y. Cao, Y. Xing, H. Hu and L. Xu, "An improved burst-mode control for VIENNA rectifiers to mitigate dc voltage ripples at light load," *2018 IEEE Applied Power Electronics Conference and Exposition* (APEC), San Antonio, TX, USA, 2018, pp. 1294-1298.

[24] P. Ide, F. Schafmeister, N. Frohleke, *et al*, "Enhanced Control Scheme for Three-Phase Three-level Rectifiers at Partial Load," *IEEE Trans. Ind. Electron.,* vol. 52, no. 3, pp. 719-726, Jun. 2005.

[25] M. Leibl, J. W. Kolar and J. Deuringer, "Sinusoidal Input Current Discontinuous Conduction Mode Control of the VIENNA Rectifier," *IEEE Trans. Power Electron.,* vol. 32, no. 11, pp. 8800-8812, Nov. 2017.

[26] H. Hu, W. Al-Hoor, N. H. Kutkut, *et al*, "Efficiency Improvement of Grid-Tied Inverters at Low Input Power Using Pulse-Skipping Control Strategy," *IEEE Trans. Power Electron.,* vol. 25, no. 12, pp. 3129-3138, Dec. 2010.

[27] Q. Zhang, W. Jiang, J. Wang, *et al*, "A Novel Modulation Method to Suppress the Current Zero-Crossing Distortion for Vienna Rectifier with Different Control Methods Under Unbalanced Grid," *IEEE Trans. Ind. Electron.,* vol. 71, no. 2, pp. 1135-1146, Feb. 2024.

[28] T. Friedli, M. Hartmann, J. W. Kolar, "The Essence of Three-Phase PFC Rectifier Systems—Part I," *IEEE Trans. Power Electron.,* vol. 28, no. 1, pp. 176-198, Jan. 2013.

[29] J. -H. Park, J. -S. Lee, M. -Y. Kim, *et al*, "Diagnosis and Tolerant Control Methods for an Open-Switch Fault in a Vienna Rectifier," *IEEE J. Emerg. Sel. Topics Power Electron.,* vol. 9, no. 6, pp. 7112-7125, Dec. 2021.

[30] T. Friedli, M. Hartmann, J. W. Kolar, "The Essence of Three-Phase PFC Rectifier Systems—Part II," *IEEE Trans. Power Electron.,* vol. 29, no. 2, pp. 543-560, Feb. 2014.

[31] Z. Zhang, G. Zhang, G. Wang, *et al*, "A Hybrid Modulation Strategy with Neutral Point Voltage Balance Capability for Electrolytic Capacitorless Vienna Rectifiers," *IEEE Trans. Power Electron* vol. 37, no. 12, pp. 14294-14305, Dec. 2022.

[32] H. Sepahvand, M. Khazraei, K. A. Corzine, *et al*, "Start-up Procedure and Switching Loss Reduction for a Single-Phase Flying Capacitor Active Rectifier," *IEEE Trans. Ind. Electron.,* vol. 60, no. 9, pp. 3399-3710, Sep. 2013.